# Results From Phase-1 and Phase-2 GOLD Experiments

K. Wilson, M. Jeganathan, and J. R. Lesh
Communications Systems and Research Section

J. James
New Mexico State University, Las Cruces

G. Xu
California Institute of Technology, Pasadena

*The Ground/Orbiter Lasercomm Demonstration conducted between the Japanese Engineering Test Satellite (ETS-VI) and the ground station at JPL's Table Mountain Facility, Wrightwood, California, was the first ground-to-space two-way optical communications experiment. Experiment objectives included validating the performance predictions of the optical link. Atmospheric attenuation and seeing measurements were made during the experiment, and data were analyzed. Downlink telemetry data recovered over the course of the experiment provided information on in-orbit performance of the ETS-VI's laser communications equipment. Bit-error rates as low as $10^{-4}$ were measured on the uplink and $10^{-5}$ on the downlink. Measured signal powers agreed well with theoretical predictions.*

## I. Introduction

The Ground/Orbiter Lasercomm Demonstration (GOLD) experiments were performed over the 7-month period extending from October 1995 to May 1996. The transmissions were broken into two phases separated by an apogee eclipse that lasted from mid-January to mid-March. A total of 44 opportunities to perform the experiments were negotiated with the Deep Space Network (DSN), National Aeronautics and Space Development Agency (NASDA), and the Communications Research Laboratory (CRL). Laser transmissions occurred every third day as the satellite's orbit brought it to apogee over JPL's Table Mountain Facility (TMF). Phase-2 transmissions were negotiated during the apogee eclipse. Access to the satellite during Phase 2 depended on NASDA's projections of the satellite's power-generating capability. These were based on measurements made during the eclipse.

Previous articles [1–3] on GOLD provide a detailed overview of the experiment hardware and operations planning. A comparison of theoretical and experimental data for one- and two-beam uplink transmissions is given in [4]. This reference also predicts the mitigation in uplink scintillation for four-beam and higher multibeam propagation.

In this article, we present the complete GOLD transmission record and describe some of the work-arounds that were implemented to address some of the difficulties encountered during the experiment.

We compare the a priori theoretical predictions of downlink performance with measurement and report on the measured uplink and downlink bit-error rates. We also report on the first extensive measurements of atmospheric seeing at TMF and briefly discuss our initial analysis of the four-beam laser uplink. Related articles published in this issue are a description of the approach used to reduce the high-speed laser communications equipment (LCE) data that were telemetered to the ground station on the optical carrier [5], the ephemeris generation process and the TMF transmitter telescope-pointing performance [6], and the calibration of the avalanche photodiode (APD) and amplifier that constitute the optical receiver [7].

## II. The GOLD Transmission Record

There were 22 opportunities to transmit to the satellite in each of the GOLD demonstration phases. Phase 1 extended from October 30, 1995, to January 13, 1996. There were 12 two-way transmissions, 1 one-way transmission, 5 cancellations due to bad weather, 2 cancellations due to hardware failures, and 2 nondetections in Phase 1. The nondetections occurred on the first two transmission opportunities as satellite and ground-station pointing strategies were being exercised. One-way transmission was detection of the uplink signal. This is shown in the pie chart in Fig. 1. Table 1 provides a brief annotation of each of the Phase-1 passes. As the table shows, the two nondetections during this phase occurred on the first two days of transmission, November 2 and 5, as we honed our ground station and satellite-pointing strategies. The hardware failure at the CRL occurred in the command control computer. The failure at TMF occurred in the transmitter facility when a short occurred in the telescope-pointing computer as a network card was being installed.

Phase-2 transmissions began on March 21, 1996, shortly after the satellite had emerged from the apogee eclipse. There were 22 Phase-2 transmission opportunities over the period from March 21, 1996, to May 26, 1996. There were 12 successful two-way transmissions, 3 one-way transmissions, 1 nondetection, 2 cancellations due to bad weather, and 3 cancellations due to satellite attitude control system (ACS) problems. The nondetections were due to the loss of the servo loop control and to the inability of the LCE to point to the ground station when the satellite was in the fixed-bias mode and ground-station pointing strategies were being exercised. One-way transmissions were detections of the uplink signal only. A synopsis of the Phase-2 transmission record is shown in the pie chart in Fig. 2, and a brief description of each pass is given in Table 2.

At the beginning of the Phase-2 experiments, we learned that the LCE's coarse-tracking servo loop that controlled the gimbal pointing had failed. Because this coarse-tracking servo controlled the acquisition of the uplink beacon, its loss was a serious blow that could have jeopardized the Phase-2

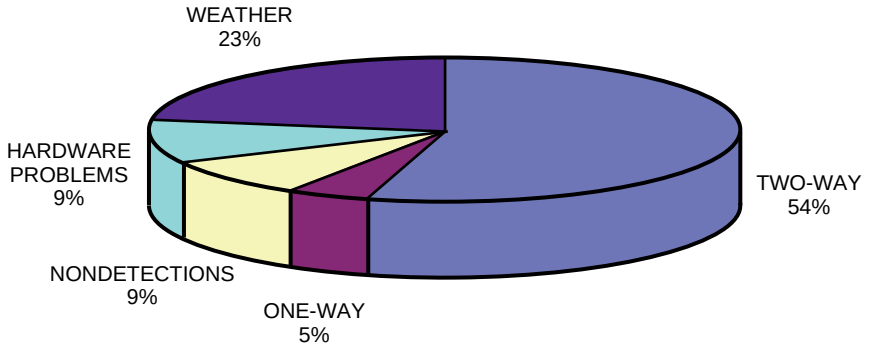


**Fig. 1. Pie chart of the GOLD Phase-1 transmission record from October 30, 1995, to January 13, 1996.**

**Table 1. Description of Phase-1 transmissions.**

| Date | Description |
|---|---|
| 10/30/95 | First scheduled uplink; overcast skies |
| 11/02/95 | Uplink not detected |
| 11/05/95 | Uplink not detected |
| 11/08/95 | Successful two-way link |
| 11/11/95 | Successful one-way link |
| 11/14/95 | Successful two-way link |
| 11/17/95 | Successful two-way link |
| 11/20/95 | Transmitter telescope computer problem |
| 11/23/95 | Thanksgiving holiday |
| 11/26/95 | Heavy cloud cover |
| 11/29/95 | Successful two-way link |
| 12/02/95 | Successful two-way link |
| 12/05/95 | Successful two-way link |
| 12/08/95 | Successful two-way link |
| 12/11/95 | Transmitter telescope not available due to schedule conflict |
| 12/14/95 | Snowing at TMF |
| 12/17/95 | Successful two-way link |
| 12/20/95 | Canceled; CRL control computer problem |
| 12/23/95 | Heavy cloud cover |
| 12/26/95 | Christmas holiday |
| 12/29/95 | Heavy cloud cover; snow storm at TMF |
| 01/01/96 | New Year's holiday |
| 01/04/96 | Successful two-way link |
| 01/07/96 | Successful two-way link |
| 01/10/96 | Successful two-way link |
| 01/13/96 | Successful two-way link |

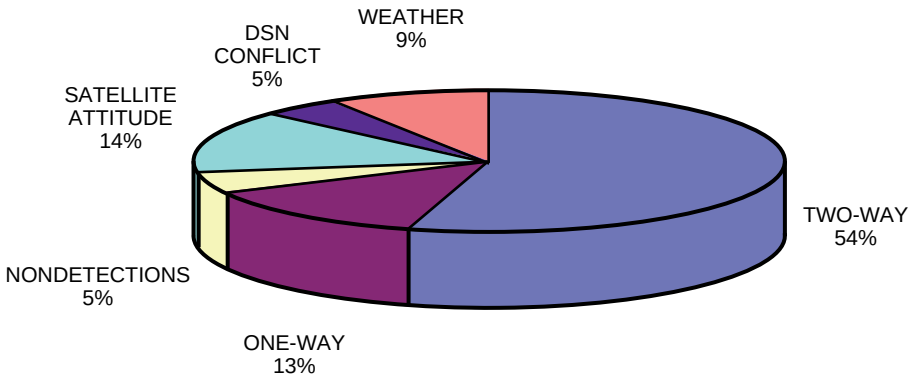


**Fig. 2. Pie chart of the GOLD Phase-2 transmission record from March 21, 1996, to May 26, 1996.**

**Table 2. Description of Phase-2 transmissions.**

| Date | Description |
|---|---|
| 03/21/96 | Successful two-way link; weak downlink |
| 03/24/96 | Cloud cover |
| 03/27/96 | No uplink or downlink detection |
| 03/30/96 | Four-beam uplink detected; no downlink |
| 04/02/96 | No transmissions; no NASDA support |
| 04/05/96 | Successful two-way link; sporadic downlink |
| 04/08/96 | Satellite put into spin-stabilized mode |
| 04/11/96 | Satellite still in spin-stabilized mode |
| 04/14/96 | Satellite still in spin-stabilized mode |
| 04/17/96 | Rain and high winds |
| 04/20/96 | Successful two-way link |
| 04/23/96 | Successful two-way link |
| 04/26/96 | Successful two-way link |
| 04/29/96 | One-way link (satellite put in fixed-attitude mode after ACS anomaly) |
| 05/02/96 | Successful two-way link |
| 05/05/96 | Successful two-way link |
| 05/08/96 | Successful two-way link but poor ephemeris file |
| 05/11/96 | Successful two-way link; daytime link accomplished |
| 05/14/96 | No DSN support; ground station antenna being modified; satellite visually tracked and telescope-pointing calibrations performed, but no transmissions possible |
| 05/17/96 | Successful two-way link |
| 05/20/96 | Successful two-way link |
| 05/23/96 | Satellite in fixed-attitude bias mode; one-way link detected |
| 05/26/96 | Successful two-way link all daytime |

demonstration. When operational, the servo automatically controlled centering the uplink signal in the field-of-view (FOV) of the LCE's charge-coupled device (CCD) camera. In so doing, it placed the signal in the narrow FOV of the quadrant detector (QD) that controlled the direction of the downlink transmission. With an operating servo loop, the delay between the uplink detection and the downlink transmission detection was on the order of a few seconds. Without the servo loop, the uplink beacon acquisition had to be performed "manually." This often took as long as 30 minutes.

With manual acquisition, the uplink beacon was acquired by scanning the LCE gimbal by single command steps over the uncertainty space of the TMF location. The uncertainty in pointing the gimbal to the ground station was compounded by uncertainties in the knowledge of the satellite's attitude bias. A combination of satellite attitude adjustment and LCE gimbal pointing was required for the LCE successfully to acquire, track, and point the downlink to the ground station. The uplink, therefore, could be detected at the edge of the CCD acquisition camera and, depending on satellite bias, be beyond the gimbal's ability to center it on the CCD. This occurred on March 30, when the satellite's attitude was unstable and the downlink transmission was not observed. We also believe that this occurred on March 27 when the uplink was not detected.

The CRL team worked on the problem of long acquisition and reacquisition times. By April 20, it had devised, implemented, and tested a gimbal-scanning routine that reduced this time from 30 minutes to about 10 minutes. The approach required that the satellite attitude be both stable and within a small

enough uncertainty to allow pointing to TMF. On April 29 and May 23, the satellite was in a fixed-attitude bias mode and uplink was detected on the edge of the CCD camera. All attempts to manipulate the gimbal to center the uplink on the CCD camera proved unsuccessful. The bias offset was too large, and the gimbal could not point the downlink to the ground station.

There were times during the course of the experiment when we would lose the uplink detection for no apparent reason. At these times, the signal on the LCE's CCD would gradually decrease to zero. When this occurred, the uplink beacon was reacquired by scanning the ETS-VI's gimbal. We suspect that this signal loss was caused by attitude disturbances on the spacecraft induced by the motion of the solar paddles as they oriented themselves to point towards the sun.

Precession in the satellite's orbit brought it above TMF approximately 15-minutes earlier on each pass. By May 26, GOLD experiments were being conducted during the day, requiring that we implement new strategies to acquire the satellite against the bright sky background. This was done by using a fast-scan routine that we had developed originally to cover the observed ephemeris errors and telescope-pointing uncertainty, errors that were as large as 1 arcminute [6]. The process of alternately scanning the uplink telescope and the LCE gimbal proved to be very successful in establishing the link. On May 26, the satellite was acquired during the day, and the link was continuously maintained for 2.5 hours of daytime operation.

## III. Downlink Signal Recovery

Two significant changes were made to the downlink signal recovery in the period between Phases 1 and 2. The first was to modify the avalanche photodiode (APD) detection circuit to operate away from gain saturation, resulting in an increase in the detection bandwidth from 1.8 to 3.8 MHz [7]. The second was to split off a portion of the AC-coupled APD signal, pass it through a squaring circuit, and measure the received downlink power. Labview software was used to sample the squared signal at 22 kHz. Using scaling factors obtained from calibration measurements, we directly converted the sampled signal to optical power for real-time display during the experiment. Real-time quantitative monitoring of the downlink signal strength proved useful as we varied both the coarse-point gimbal and point-ahead mirrors on the LCE to optimize the downlink signal pointing.

A plot of the measured and a priori predicted signal strengths in Fig. 3 shows that the measured downlink signal strength was within the ±3-dB uncertainty of the a priori theory. Our a priori assumptions were 60-percent atmospheric transmission and 5 microradians pointing uncertainty. The error bars on the measured data (triangles) represent the standard deviation in the measured downlink signal strength. The circles in Fig. 3 are the corrected theoretical values based on the atmospheric transmission measured by the autonomous visibility monitoring station at TMF.

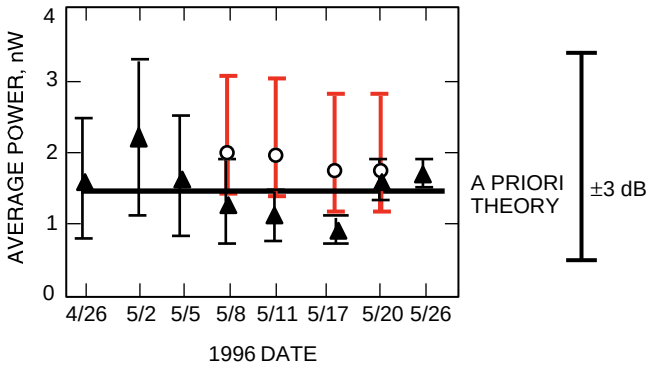


**Fig. 3. Comparison of theoretical prediction and measurement of downlink power at a 1.2-m receiver.**

There were three operating modes for the downlink optical transmission. These were (1) a 511-bit-long pseudorandom noise (PN) sequence, (2) 128-kbps LCE telemetry (E2), and (3) regeneration of a 1-Mbps uplink data sequence. Switching between downlink telemetry modes was accomplished in seconds. The spectra for the three modes were quite distinct, and the switch from one mode to another was readily monitored by using the spectrum analyzer feature of the DSA 602A oscilloscope. We used this approach in postdetection processing to identify the time intervals when specific downlink modes, PN, or E2 data were transmitted. This allowed us to go to the data stored on magnetic Exabyte tapes and locate those time segments on the recorded telemetry.

Figures 4 and 5 are fast Fourier transforms (FFTs) of the downlink power fluctuation measured using the APD squaring circuit. The spectra represent an average over 50 minutes of downlink transmission. In both figures, the power spectrum rolls off around 10 kHz, consistent with the Nyquist criteria for a 22-kHz sampling rate. Figure 4 is the FFT of the E2 data stream. It shows a distinct peak at 8 kHz, the frequency of an overlayed amplitude modulation that was impressed by the LCE on the optical downlink. Also evident are the spectral peaks at 500-Hz intervals, corresponding to the 2-millisecond-long E2 frame of 2048 bits [5]. The side bands on the 500-Hz spectra are not in all of the FFTs for the various days, and are unexplained at this time. One possible explanation could be instabilities in the satellite's electronic circuitry.

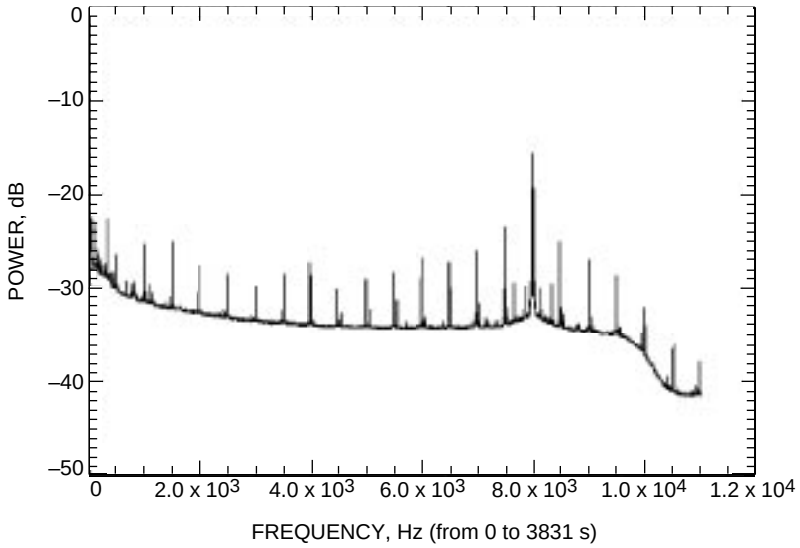


**Fig. 4. The FFT of the E2 data stream recovered on May 11, 1996, showing the spectral peaks at 500-Hz intervals, corresponding to the 2-ms-long E2 data frame.**

Figure 5 is an FFT of the received downlink PN data stream. It shows spectral peaks at 2-kHz intervals. This corresponds to the 2.004-kHz repetition frequency of the 511-bit-long PN sequence in the 1.024-Mbps data stream. Again, the figure shows the strong peak at 8 kHz. This is the superposition of the harmonics of the PN spectrum and the 8-kHz amplitude modulation of the laser power that was impressed on the optical downlink.

The downlink telemetry data were bit synchronized and recorded for postdetection demodulation and processing. The PN data were processed to determine the bit-error rates (BERs) on the downlink. Figure 6 shows a 3-minute-long segment of the downlink BER measurements that were demodulated from the PN data stream. Each data point represents 200 frames or 100 milliseconds of data. The figure shows that the bit errors occur in bursts and that several frames were error free (i.e., BERs as low as $10^{-5}$). Also seen are times at which the link appeared bursty, with very high BERs. Possible causes are

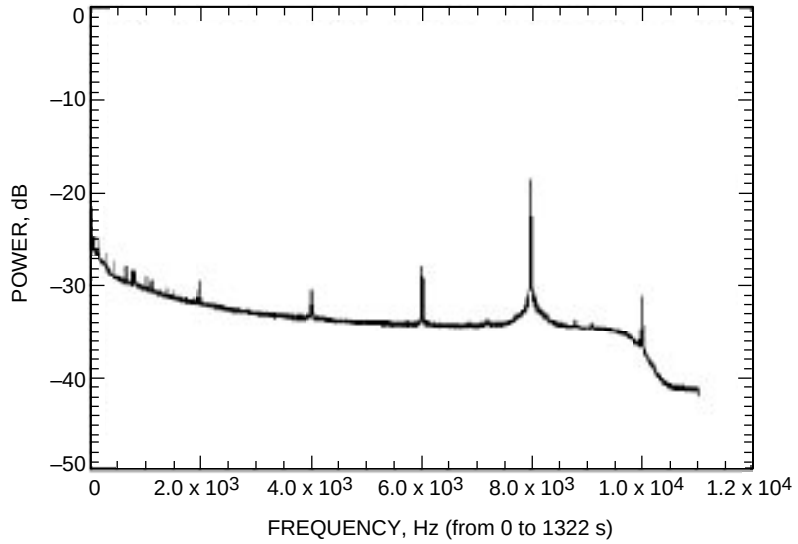


**Fig. 5. The FFT of the PN downlink data recovered on May 17, 1996, showing a 2-kHz interval spectrum, corresponding to the 2.004-kHz repetition frequency of the 511-bit-long PN sequence in the 1.024-Mbps data stream.**

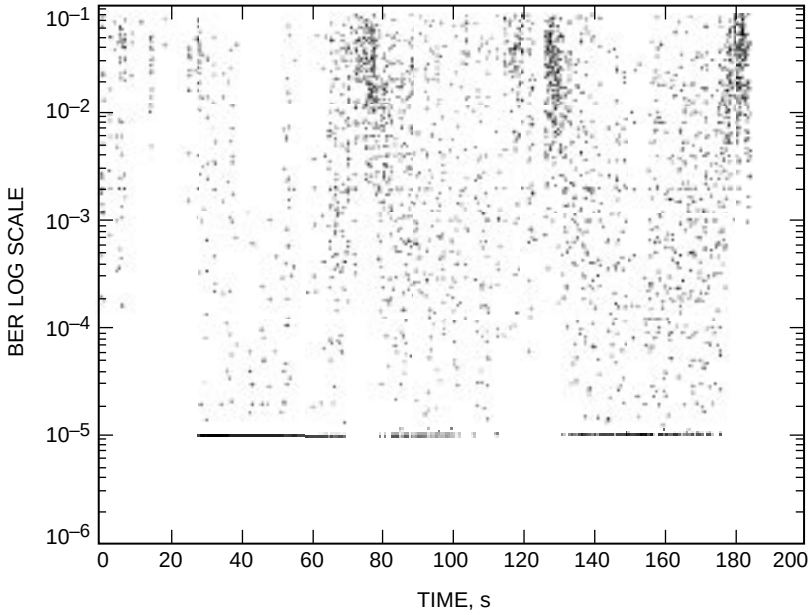


**Fig. 6. The BER measured in a 3-min-long PN data sequence on April 27, 1996. Each point represents 0.1 s of data at 1.024 Mbps.**

bit-synchronization errors on the downlink detection, errors in the transmitted telemetry, or fluctuations in the downlink power due to unstable tracking of the uplink beacon by the LCE. The BER distribution in Fig. 6 is not expected to be a representative sample of the data from the entire GOLD experiment. We often observed that the downlink pointing was less than optimum during the experiment. Yet, demodulation of these data could provide valuable information on the LCE performance over the GOLD demonstration period.

## IV. Uplink Signal Detection

Multibeam propagation was extended from two beams during Phase 1 to four beams during Phase 2. There was good agreement between experiment and theory for the one-beam and two-beam propagation measurements observed during Phase 1 (see [3]). Preliminary analysis of the four-beam uplink validated the predicted reduction in uplink signal variance.

Uplink bit-error rates are most susceptible to atmospheric seeing conditions where the scintillation and beam wander result in deep fades and bursty signals. We uplinked a 1.024-Mbps Manchester-coded, 511-bit-long PN sequence to the satellite to measure the uplink BER. Measurements were made using the onboard bit-error rate tester (BERT) to count the number of errors in a 1-second interval. Initiation of the test interval was marked by transmitting to the satellite a symbol sequence of ones that was then followed by the PN transmission. The measured BERs were relayed to the ground on the S-band (2.3-GHz) downlink telemetry. The results of nine such 1-second measurements are given in Table 3. The measurements were made with a two-beam uplink over a 40-minute period on January 4. The table shows uplink bit-error rates on the order of $10^{-3}$ and $10^{-4}$. The measured mean atmospheric seeing for the night was measured at 2 arcseconds (see Fig. 7).

**Table 3. Uplink bit-error rates in 1-second intervals.**

| Time | BER |
|---|---|
| 20:10:17 | $2.49 \times 10^{-3}$ |
| 20:13:55 | $2.28 \times 10^{-3}$ |
| 20:13:56 | $2.49 \times 10^{-3}$ |
| 20:18:11 | $1.19 \times 10^{-3}$ |
| 20:18:12 | $2.49 \times 10^{-3}$ |
| 10:36:49 | $8.01 \times 10^{-4}$ |
| 20:36:50 | $2.49 \times 10^{-3}$ |
| 20:52:19 | $3.61 \times 10^{-4}$ |
| 20:52:20 | $2.49 \times 10^{-3}$ |

## V. Atmospheric Seeing Measurements

Figures 7 and 8 show the atmospheric seeing measurements recorded during the GOLD experiment. Atmospheric turbulence caused by temperature and pressure variations in the atmosphere results in scintillation of the light from a point source as it propagates through the atmosphere. On the downlink, this effect is averaged out over large ground receiving apertures. On the uplink, however, turbulence causes both scintillation and beam wander (tilt) in a laser beam transmitted from a ground station to a spaceborne receiver. These effects, if left uncompensated, are manifested as fades and surges in the uplink signal, resulting in high bit-error rates in the uplink communications data stream.

Seeing measurements were made at 15-minute intervals from a 1.2-m receiver telescope using a Spectra Source slow scan CCD camera. The CCD camera was coaligned with the APD, and the detected downlink signal was integrated for several seconds. The atmospheric seeing was determined from the full-width-at-half maximum of the measured intensity distribution on the CCD array.

Figure 7 shows that seeing during Phase 1 typically was between 1.5 and 3 arcseconds at the 2-km-high TMF site. These experiments were conducted at night between 10 p.m. and 4:00 a.m., when

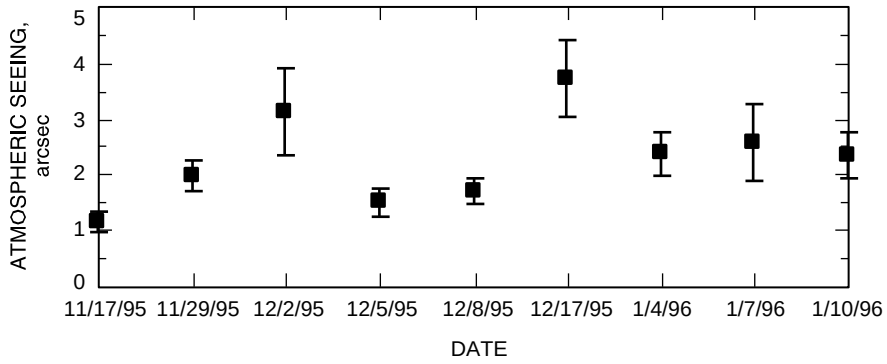


**Fig. 7. Measured atmospheric seeing during the Phase-1 GOLD demonstration.**

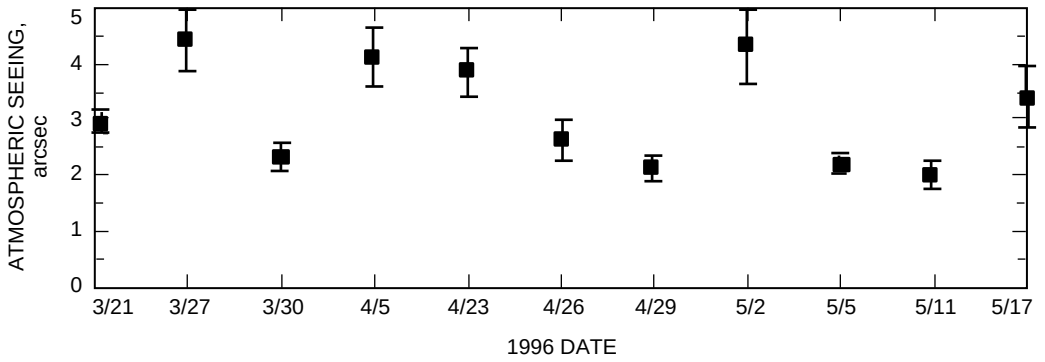


**Fig. 8. Measured atmospheric seeing during the Phase-2 GOLD demonstration.**

the turbulence was low. Phase-2 experiments were conducted during the afternoon and early evening, periods of high atmospheric turbulence. Seeing during Phase 2 was much worse than during Phase 1 (Fig. 8), and on certain days was as high as 4 or 5 arcseconds. Except for March 27, when a bright star was used, all seeing measurements were made by integrating the downlink signal for several seconds on a slow-scan CCD camera.

## VI. Conclusion

GOLD is the first successful demonstration of two-way optical communications with a satellite. The results presented in this article cover the spectrum of data types acquired during the demonstration. The downlink telemetry data presented here represent a small fraction of the total data that were recovered during GOLD. We have presented results of BERs on both the uplink and the downlink transmissions. The recovered downlink telemetry on the optical carrier represents the only high data-rate record of the LCE's performance. The data recovered have validated our models for the optical downlink and also have provided insight into the performance of both the optical link and the LCE. Our models for multibeam uplink have validated the predicted advantages of multi-beam transmission over single-beam transmission.

## Acknowledgments

The authors would like to acknowledge the contributions of all of the other GOLD team members. We would like especially to acknowledge the assistance of Y. Arimoto, K. Araki, M. Toyoshima, M. Toyoda, and the members of their CRL staff who spent several long nights and days supporting this experiment. We also would like to acknowledge Y. Arimoto and K. Araki for providing the uplink BER data presented in Table 3 of this article.

## References

[1] K. E. Wilson, "An Overview of the GOLD Experiment Between the ETS-VI Satellite and the Table Mountain Facility," *The Telecommunications and Data Acquisition Progress Report 42-124, October–December 1995*, Jet Propulsion Laboratory, Pasadena, California, pp. 8–19, February 15, 1996.
http://tda.jpl.nasa.gov/tda/progress_report/42-124/124I.pdf

[2] K. E. Wilson, J. R. Lesh, K. Araki, Y. Arimoto, "Preliminary Results of the GOLD (Ground Orbiter Lasercomm Demonstration) Experiment Between Table Mountain Observatory and the ETS-VI Satellite," *SPIE Proceedings*, San Jose, California, vol. 2699, pp. 121–132, January 1996.

[3] K. E. Wilson, "Preliminary Results, Analysis and Overview of Part-I of the GOLD Experiment," Invited Paper, CRL International Symposium on Advanced Technologies in Optical Communications and Sensing, Tokyo, Japan, March 13, 1996.

[4] M. Jeganathan, K. Wilson, and J. R. Lesh, "Preliminary Analysis of Fluctuations in Received Uplink-Beacon-Power Data Obtained From the GOLD Experiments," *The Telecommunications and Data Acquisition Progress Report 42-124, October–December 1995*, Jet Propulsion Laboratory, Pasadena, California, pp. 20–32, February 15, 1996.
http://tda.jpl.nasa.gov/tda/progress_report/42-124/124J.pdf

[5] M. Toyoshima, K. Araki, Y. Arimoto, M. Toyoda, M. Jeganathan, K. Wilson, and J. Lesh, "Reduction of ETS-VI Laser Communication Equipment Optical-Downlink Telemetry Collected During GOLD," *The Telecommunications and Data Acquisition Progress Report 42-128, October–December 1996*, Jet Propulsion Laboratory, Pasadena, California, pp. 1–9, February 15, 1997.
http://tda.jpl.nasa.gov/tda/progress_report/42-128/128I.pdf

[6] W. M. Owen, Jr., S. D. Gillam, J. W. Young, and D. Mayes, "Ephemeris Generation for ETS-VI and Its Effects on Pointing Strategies Adopted for Daytime Acquisition and Tracking," *The Telecommunications and Data Acquisition Progress Report 42-128, October–December 1996*, Jet Propulsion Laboratory, Pasadena, California, pp. 1–11, February 15, 1997.
http://tda.jpl.nasa.gov/tda/progress_report/42-128/128L.pdf

[7] C. Pasqualino, "Characterization of the Avalanche Photodiode Detector Used for Optical Communications Experiments With the Japanese ETS-VI," *The Telecommunications and Data Acquisition Progress Report 42-128, October–December 1996*, Jet Propulsion Laboratory, Pasadena, California, pp. 1–8, February 15, 1997.
http://tda.jpl.nasa.gov/tda/progress_report/42-128/128J.pdf